Mixing enthalpies of fluorinated precursors for textile industry in ionic liquids

Guillaume Simon, Jocasta Avila, Agílio Pádua, Margarida Costa Gomes

Mixing enthalpies of fluorinated precursors for textile industry in ionic liquids

Guillaume Simon*, Jocasta Avila*, Agilio Padua*, and Margarida Costa Gomes**

Laboratoire de Chimie de l'ENS Lyon, École Normale Supérieure de Lyon & CNRS, 69364 Lyon Cedex 07, France

E-mail: margarida.costa-gomes@ens-lyon.fr

Abstract

Per- and polyfluoroalkyl substances (PFAS) are widely used for technical purposes in textile finishing, giving water or oil repellence to the fibres. During their production, textile manufacturing or consumer-use, these additives can be degraded into their precursors and released in the environment. These substances are volatile, bio accumulative and persistent, and their release in the environment is more and more regulated in the EU . For a textile recycling purpose, it is necessary to find ways to safely remove them from the fibres. Among other alternative solvents, ionic liquids showed solvation properties that are promising for recycling textile waste. We have used the COSMO-SAC modelling approach to screen a large number of ionic liquids and, by the calculation of infinite dilution activity coefficients, find the most appropriate solvents for two representative fluorinated precursors likely to be found in textile products. We could determine which ionic liquids were able to interact favourably with perfluorobutyric acid (PFBA) and 6:2 fluorotelomer alcohol (6:2 FTOH). These information could be quantified using isothermal titration calorimetry (ITC) for PFBA in 1-butyl-3-metylimidazolium bis(trifluoromethylsulfonyl)imide, $[C_4C_1Im][NTf_2]$, predicted

by COSMO-SAC as a weak solvent, as well as in 1-ethyl-3-methylimidazolium methylsulfonate, $[C_2C_1Im][MeSO_3]$ and 1-butyl-3-methylimidazolium acetate, $[C_4C_1Im][OAc]$, expected to have strong interactions with the textile additive. Mixing enthalpies of 6:2 FTOH were measured in selected ionic liquids, namely triethylammonium methylsulfonate, $[N_{222}H][MeSO_3]$, 1-ethyl-3-methylimidazolium methylsulfonate, $[C_2C_1Im][MeSO_3]$ and acetate, $[C_2C_1Im][OAc]$. A proton transfer from PFBA to AcO^- – and to a lesser extent from 6:2 FTOH to AcO^- – was investigated and described with DFT calculations, ^{1}H NMR analysis and FT-IR spectroscopy.

Introduction

In textile industry, liquid repellency is a property valuable for many types of garments. Common outdoor apparels are often meant to be water-repellents, but other clothes including technical garments can require more and higher levels of protection. For example, medical textiles have to be repellent to biological fluids, and military or fire-fighters garments have to preserve from oil or chemicals.[1]

These requirements led to the use of polymeric fluorinated additives, because of their ability to change the surface properties of the products they are applied on. Per- and polyfluoroalkyl substances (PFAS) are a vast class of chemicals, with an estimation of more than 3000 commercialised products.[2,3] They were found to have a very low surface energy, so the treatment of textiles with such chemicals lowers the one of the fabrics, and reduces their wettability.[4]

PFAS terminology refers to either *per*-fluoroalkyl substances (*i.e.* all H attached to *all carbons* in the original substance are replaced by F) or *poly*-fluoroalkyl substances (*i.e.* all H attached to *at least one carbon* in the original substance are replaced by F) and designates both non-polymeric and polymeric fluorinated compounds.[5]

Within the scope of textile industry, non-polymeric PFAS are commercialised as either aids for the production of fluoropolymers or as precursors for the synthesis of other flu-

orinated polymers.[6] These moieties are **fluorotelomers** ($F(CF_2)_n(CH_2)_2R$) and **perfluoroalkyl organics** ($F(CF_2)_nR$) derivatives. Until 15 years ago, PFAS were mostly "highly fluorinated" or "long-chain PFAS" (*i.e.* $n \geq 7$) and the most used were perfluorooctanoic acid (PFOA), perfluorooctanesulfonic acid (PFOS), 8:2 fluorotelomer alcohol (8:2 FTOH) and 8:2 fluorotelomer (meth)acrylate (8:2 FT(M)Ac).

The main polymeric PFAS used in textiles are **side-chain fluorinated polymers (SFP)** and **fluoropolymers**. The substances of the first category are composed of a non-fluorinated backbone and side-chains derived from cross-linked fluorotelomers (mainly FTOH and FT(M)AC). These repellents are applied to textiles as impregnating agents forming a thin protective film by curing process.[6] The Swedish Chemicals Agency counted fluorinated (meth)acrylate polymers as having the highest number of substances on the global market of PFAS.[2] During years, 3M commercialised long-chain fluorinated coatings like the PFOA-based *Scotchgard®*.

Non-polymeric PFAS, and especially PFOA, can be discharged in the environment. In 2006, it was already estimated that approximately 80% of the perfluorocarboxylic acids had been released from fluorinated polymers.[7] There are three different routes for non-polymeric PFAS release: during the production of the repellents, as residuals in the final consumer goods, or by the degradation of the polymers.[5]

The highest volumes of PFAS released in the environment come from the production and finishing stages of textile manufacturing, but a non-negligible quantity escapes from the final goods.[7,8] Residual volatile compounds like fluorotelomers can evaporate into the atmosphere, be washed out to the soil by rain, or lost into wastewater during laundering.[9] Fluoropolymers themselves do not easily degrade to PFAS moieties, but residual aids to their synthesis, mostly PFAA, can follow the same release pathways than the ones just described for fluorotelomers. Finally, it was proved that SFP are the polymers the most likely to degrade, because of weathering and laundering,[8,10,11] as the ester linkages between the backbone and the fluorinated side-chains are breakable.

Because of fluorine atoms, PFAS – and especially long-chain PFAA – are highly stable and persistent in the environment, so that they are popularly called "*forever chemicals*".[12] Ionic PFAA are water-soluble and highly volatile, so they can easily be transported in water or the atmosphere[13] and were even found in polar regions.[14] As they are able to bind to proteins,[3] PFAS are bioaccumulative[15] and are slowly eliminated by human body.[16] This bioaccumulation is fueled by their persistence and transport over time. Health concerns about PFOA exposure were raised, as its hepatotoxicity – causing liver damages – was shown,[17] but also its deregulation effect on the reproduction of animal subjects.

Several environmental and toxicological studies led governments and institutions to ban such chemicals. In 2006, the European Commission regulated the production of PFOS[18] and the substance and its derivatives were listed in the Stockholm Convention in 2009 (decision SC-4/17), which restricted globally their production and use. In 2017, PFOA was classified as substance of concern in REACH[19] and was also globally added to the Stockholm Convention (decision SC-9/12). European Union planned to extend the restriction to C9-14 perfluorocarboxylic acids in February 2023.[20]

After this regulation, the main PFAS manufacturers phased out the production of PFOS and PFOA and had to find alternatives[1] for the synthesis of liquid-repellents. Several non-fluorinated susbtances have been tested, like paraffin emulsions, silicone-based polymers, hyperbranched dendrimers, and coatings based on SiO_2 or AlO_3 nanoparticles.[21] These alternatives were found to be water-repellent, but not as much as long-chain SFP, and not oil-repellent.[22] Manufacturers actually moved to short-chain (C_6 or less) fluorinated repellents, which were shown to be less persistent than their long-chain counterparts while providing oil-repellency.[1]

The total regulation of PFOA is quite recent, and even if its production was phased out, PFAS-based repellents are still used in textile industry. As fluorotelomers and perfluorocarboxylic acids precursors might be present as residues or degradation products of the polymers, we believe that the recycling processes of textile waste have to take their presence

into account, and avoid their release into wastewater. Studying interactions between fluorinated precursors and solvents for textile recycling is the first step to address their capture in the above-named solvents.

Ionic liquids are known to interact with fluorinated compounds. This class of alternative solvents is composed of salts having a melting point near room temperature. Usually this assessment includes salts liquid from below room temperature up to 100°C, even if this upper border is subject to discussion.[23] Whether ionic liquids are liquid below or above 100°C is not capital, as their applications can require temperatures above this limit and still benefit from their unique properties.

Unlike conventional inorganic salts, ILs have a decreased melting temperature due to the pairing of large, asymmetric, organic cations – usually imidazolium, pyrrolidinium, pyridinium, ammonium, phosphonium and sulfonium – with a wide range of organic or inorganic anions. Their structure allows charge delocalisation and prevents crystallisation.[24] It is possible to design the ions by several methods like atomic susbtitution, functionalisation or the grafting of alkyl chains. This implies the existence of more than 10^6 potential ionic liquids,[25] and postulates that any application can use at least one ionic liquid with tuned properties.

In comparison with conventional solvents, ILs have negligible vapour pressures at atmospheric temperature. They are almost non-volatile, often non-flammable, and in many cases have excellent conductivities and thermal stabilities. Their non-volality/flammability and the fact that it is possible to regenerate them – when used as solvents for volatile compounds – can put them into the category of green solvents, even if their non-toxicity was not always proved.[25] But as it was highlighted before, there is an almost unlimited range of ionic liquids, so it is possible to design non-toxic and biodegradable ILs matching desired functional properties.

These chemicophysical characteristics, added to their ability to form diverse electrostatic, van der Waals and H-bonding interactions, raised them as interesting alternative solvents. They are already used at a commercial or pilot scales for electrochemical applications, or as

alkylation or hydrogenation catalysts, gas capture, lubricants, and above all – for our present interest – solvation and extraction media.[25] They are also a solvation medium for organic compounds like dyes or pharmaceuticals,[26] which encourages to use them for the extraction of textile additives such as PFAS.

Ionic liquids are used for the capture of fluorinated cooling gases – described as greenhouse gases[27] – prior to their treatment or recycling. Phosphonium-based ILs proved their ability to absorb CF_4, C_2F_6, C_3F_8[28] and more recently imidazolium ionic liquids raised an interest for F-gases absorption. These cations combined with the fluorinated counterpart of long-chain hydrogenated anions demonstrated selectivity towards gas mixtures.[29] Imidazolium-based ILs with carboxylate and sulfonate anions are also promising solvents for common F-gases capture.[30]

Recently, ionic liquids were also used for the liquid-liquid extraction of PFAS – mainly PFOA – from wastewater. In this processes, an issue remains to be solved as the PFAS can cause the emulsification of the extractants, which limits the final concentration of the extracted solutes. The use of ammonium-based ionic liquids, associated with NTf_2^- anion (e.g. $[N_{1888}][NTf_2]$) and diluted in n-octanol, could avoid this phenomenon.[31] Without the use of a diluent, an appropriate choice of the PFOA:IL molar ratio was also found to be efficient to limit emulsification. The non-fluorinated $[P_{66614}]$[Piv] – pivalate anion being named by IUPAC 2,2-dimethylpropanoate – was proved to be the best ionic liquid when only mixed with PFOA-containing wastewater.[32] COSMO models were also used to calculate the infinite dilution activity coefficient $ln\gamma^{\infty}$ of PFOA in water + ILs mixtures[32,33] and to predict the most promising solvents, showing that the anion plays the most important role in PFOA extraction[32] by the presence of a H-bond acceptor.[33]

In the present work, we want to provide an understanding of the interactions between ionic liquids and fluorinated precursors of textile water-repellents, namely perfluorobutyric acid (PFBA) and 6:2 fluorotelomer alcohol (6:2 FTOH). Because numerous combinations of cations and anions are possible when preparing ionic liquids, a previous *in silico* screening

is an interesting approach. This screening can be performed for example using Conductor-like Screening Model (COSMO)-based methods. Although COSMO-RS and COSMO-SAC variants have been already used for the prediction of gas solubility in ionic liquids,[34] phase behavior of ILs[35,36] or the solubility of organic solutes,[37–39] a few publications so far has used this screening tool to assess the affinity of PFAS in pure ionic solvents.[32,33] We designed ionic liquids to have favourable interactions with PFBA and 6:2 FTOH on the basis of a two-step strategy: first, by *in silico* screening of a large number of salts using the COSMO-SAC method with the calculation of infinite dilution activity coefficients of the chosen PFAS in ionic liquids; and second, studying experimentally some ILs, through the direct quantification of their interactions of the chosen PFAS, namely the measurement of mixing enthalpies with isothermal titration calorimetry.

In silico screening of ionic liquids

The chemical potential μ_i of a compound in a mixture can be defined as

$$\begin{aligned} \mu_i &= \mu_i^* + RT.ln(\gamma_i x_i) \\ &= \mu_i^* + RT.lnx_i + RT.ln\gamma_i \end{aligned} \tag{1}$$

where μ_i^* is the chemical potential of the pure compound, x_i its mole fraction and γ_i its activity coefficient. In an ideal mixture, the interactions between the compounds are equivalent to those in the pure compounds. The activity coefficient $\gamma = 1$, the chemical potential only depends on the properties of the pure compounds and the composition of the mixture. The contributions from the other compounds are all contained in the activity coefficient γ.

In a non-ideal mixture, the interactions between the compounds are not equivalent to the interactions in the pure compounds and the activity coefficient of each component is different from 1. The activity coefficient is then a convenient way of comparing different solvents for

their solvation ability. If $\ln \gamma < 0$, the deviation from ideality is negative meaning that the interactions between solute and solvent are more favourable than the interactions in the pure compounds. The more negative $\ln \gamma$ is, the more soluble a compound is expected to be in a given solvent.

With COSMO-based (COnductor-like Screening MOdel) methods, a molecule of solute is assumed to be in a dielectric continuum conductor, forming a cavity. By the calculating the van der Waals-like interaction energies in numerous points in the cavity,[40] it is possible to obtain the surface charge densities of the compound. The charge distributions can also be represented as two-dimensional histograms, the σ-profiles, where the area is represented as a function of the surface charges. In these σ-profiles the H-bond donor/acceptor regions of the molecules are represented, as negative and positive surface charges, respectively.

In a mixture, the interactions between two compounds induce a change in the calculated energy and surface charge distribution. In the COSMO-SAC (Segment Activity Coefficient) method, the molecular surfaces are divided into segments, and the probability of contact between each pair of segments is calculated following a statistical approach.[41] From these calculations, it is possible to assess the activity coefficients of each segment and, from there, the activity coefficients of the species in the mixture. At infinite dilution, one molecule of solute is surrounded only by molecules of solvent. So the calculations of infinite dilution activity coefficients ($\ln \gamma^{\infty}$) allow to focus only on solute-solvent interactions and so to predict which species constitute a promising solvation environments for a given compound. It is possible to have a first look on affinities by the comparison of the σ-profiles of the solute with the different solvents. Qualitatively, a compound should have more favourable interactions in a solvent with a σ-profile that overlaps with its own.

The geometries of the fluorinated precursors and ionic liquids (cations and anions) were optimized with Gaussian 09 package, using B3LYP/6-31++G (d) level. The structures of the PFAS are shown in Figure 1. The σ-profiles were then calculated with the GAMESS package, using triple zeta KTZVP basis. The σ-profiles were implemented in the LVPP

JCosmo package[42] for the calculation of $\ln \gamma^{\infty}$ at a set temperature of 298 K. The cations and anions constituting the ionic liquids were treated as separate components at equimolar proportions and the mole fractions of the solutes were taken as zero to model infinite dilution state. For each fluorinated substance, $\ln \gamma^{\infty}$ were calculated for 22 anions and 42 cations, for a total of 924 potential ionic liquids. Two-factors ANOVA calculations were made, with anion and cation as factors, to estimate the dominant contribution in the values of $\ln \gamma^{\infty}$.

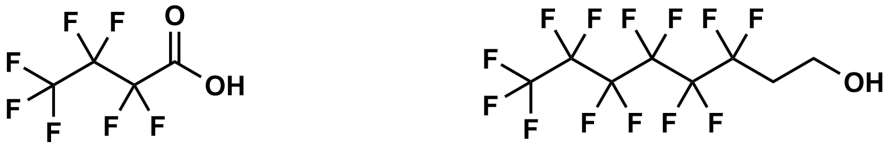

PFBA
Perfluorobutyric acid

6:2 FTOH
6:2 Fluorotelomer alcohol

Figure 1: Molecular structures of the studied PFAS

Experiments

Theoretical background

Enthalpy of mixing is the enthalpy change upon mixing, in relation with the energy due to the interactions between the components of a system. For non-ideal mixtures the mixing enthalpy can be defined as:

$$\Delta_{mix}H = \Delta_{mix}H^{id} + H^{E} \tag{2}$$

where $\Delta_{mix}H^{id}$ is the enthalpy of mixing of an ideal mixture and H^{E} the excess enthalpy, which represents the deviation of enthalpy from ideality.

As the enthalpy of mixing of an ideal mixture is equal to zero, we can assume that:[43]

$$\Delta_{mix}H \equiv H^{E} \tag{3}$$

When $\Delta_{mix}H < 0$ (exothermic process), in a A+B mixture, the A-B interactions are more

favourable than the average of A-A and B-B and they contribute to spontaneous mixing. If the behaviour is endothermic ($\Delta_{mix}H > 0$) the interactions are energetically less favourable for spontaneous mixing.

In this paper, we will always denote the *molar* value of excess enthalpy as H^E. We will use H^E ($\equiv \Delta_{mix}H$) as a comparison of the affinity between ionic liquids and fluorinated substances. By measuring molar excess enthalpies of mixtures composed of per/polyfluoroalkyl substances in different ionic liquids, we can describe how strong the interactions PFAS/ILs are as compared with the interactions in the pure compounds and then establish which ionic liquids are the most suitable for the capture of F-additives during textile recycling. The more negative molar excess enthalpies are, the bigger contribution they bring to spontaneous mixing.

A way to access mixing enthalpy is a direct measurement of molar excess enthalpy.[43] We can define $\overline{H}_i^E$ the partial molar excess enthalpy of a component i as the *change* to the excess enthalpy (nH^E) when n_i is *added* to the mixture, at constant pressure, temperature and amounts of components j:

$$\overline{H}_i^E = \left(\frac{\partial(nH^E)}{\partial n_i}\right)_{p,T,n_{j\neq i}} \tag{4}$$

With the assumption done at the equation 3, in a system A+B, the total mixing enthalpy can be related to the partial molar excess enthalpy of a solute B in a solvent A with:

$$\overline{H}_B^E = \left(\frac{\partial(n_A + n_B)\Delta_{mix}H}{\partial n_B}\right)_{p,T,n_A} \tag{5}$$

and vice versa if A is added into B. The value of $\overline{H}_i^E$ can be directly measured using the isothermal titration calorimetry (ITC).

Two chambers (reference and sample) contain one component of the mixture (usually the solvent) and are housed in a thermostat maintained at constant temperature with an accuracy better than 1 mK. In the sample chamber, a small quantity – relatively to the

volume of the chamber – of the solute is injected with a high precision syringe and generates a heat transfer upon mixing.

Using the principle of heat flow acquisition, the calorimeter measures the power required to compensate (increase or decrease) the temperature change due to the heat transfer. The compensation is acquired as a response peak, whose the orientation depends on the exothermicity (heat released) or endothermicity (heat absorbed) of the process. The area of the peaks corresponds to the heat Q_i due to the addition of i. When a very small quantity of one substance is injected into a much larger volume of the other component, we can assume that the process reaches equilibrium as followed by the recovery of the baseline signal of the calorimeter. We can approximate the partial molar excess enthalpy due to an addition of a small quantity of the substance i:

$$\overline{H}_i^E = \frac{Q_i}{\Delta n_i} \tag{6}$$

where Q_i is the heat due to the addition of a quantity Δn_i of the solute i.

By performing this measurement at several compositions of the mixture, and fitting the experimental values in a Redlich-Kister (RK) polynomial equation, here for a mixture A+B with B the solute:

$$\begin{aligned} \overline{H}_B^E &= \Delta_{mix}H + (1 - x_B)\left(\frac{\partial \Delta_{mix}H}{\partial x_B}\right)_{p,T,x_A} \\ &= (x_B - 1)^2\left(x_B \sum_{i=0}^{n} -2iA_i(1 - 2x_B)^{-1+i} + \sum_{i=0}^{n} A_i(1 - 2x_B)^i\right) \end{aligned} \tag{7}$$

where x_B is the molar fraction of B and A_i the RK polynomial parameters.

By integration of equation 7 with respect to composition, it is possible to obtain the mixing enthalpy, or molar excess enthalpy, of the mixture and conclude about the A-B interactions:

$$\Delta_{mix}H = x_B(1 - x_B)\sum_{i=0}^{n} A_i(1 - 2x_B)^i \quad (8)$$

From the equation 7 extrapolated to $x_B \to 0$, we can also get the value of partial molar excess enthalpy of the solute B at infinite dilution:

$$\overline{H}_B^{E,\infty} = \lim_{x\to 0} \overline{H}_B^E = \sum_{i=0}^{n} A_i \quad (9)$$

The experimental results fitted to equations 8 and 9 will provide information about how the interactions between PFAS and ionic liquids are contributing to spontaneous mixing and what the energetic behaviour is at infinite dilution.

Materials

PFBA (Heptafluorobutyric acid, 99%) and 6:2 FTOH (1H,1H,2H,2H-Perfluoro-1-octanol, 95%) were bought from Alfa Aesar. 1-Butyl-3-methylimidazolium bis(trifluoromethylsulfonyl)imide ($[C_4C_1Im][NTf_2]$) was synthesized by a collaborator of our research group and all the other ionic liquids ($> 97\%$) were purchased from IoLiTec (see figure 2).

Prior to ITC and density measurements, $[C_2C_1Im][MeSO_3]$ and $[C_4C_1Im][NTf_2]$ were dried under primary vacuum during several days. The ionic liquids $[C_2C_1Im][OAc]$, $[C_4C_1Im][OAc]$ and $[N_{222}H][MeSO_3]$ were degassed with the freeze-pump-thaw cycling method, to avoid forming acetic acid during primary vacuum drying, or causing proton transfer in $[N_{222}H][MeSO_3]$, facilitated by water evaporation. Cycles of liquid nitrogen-freezing + pump degassing were performed until no gas bubble could be seen upon stirring and no change of pressure was registered when opening to vacuum. In total, 7 to 10 cycles were necessary to dry the ionic liquids. The same method was applied to PFBA, whereas 6:2 FTOH was dried with molecular sieves (4Å). The water content of all the chemicals was measured with a Mettler Toledo CS20 Karl Fischer coulometric titrator after their drying or degassing process and they were stored under argon in a vial.

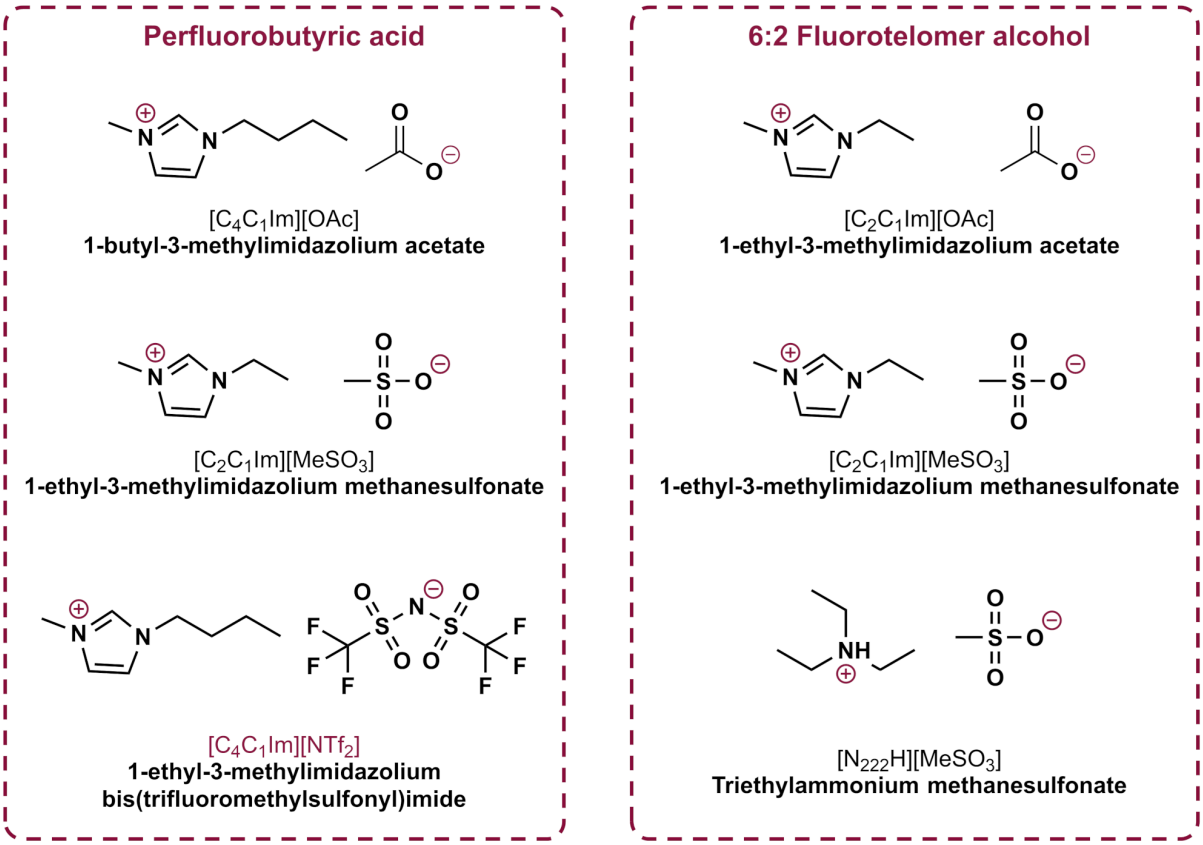

Figure 2: Structures of the ionic liquids used to study experimentally the solubility of the fluorinated solutes.

Isothermal Titration Calorimetry experiments

The partial molar excess enthalpy $\overline{H}_i^E$ of PFBA+IL and 6:2 FTOH+IL were measured at several compositions, at $298.15K$ or $313.15K$ and at atmospheric pressure. The calorimetric experiments were performed in an isothermal titration nanocalorimeter (TA Instruments) housed in a Thermal Activity Monitor TAM IV thermostat (TA Instruments). Table 1 shows the details about the ionic liquids, the compositions at which the heat effects were measured, the number of injections and the temperature for each system.

For each experiment, measuring and reference stainless steel cells of 1 mL were filled with 0.7 mL of one of the pure compounds (ionic liquid or F-substance), or with mixtures of known composition as detailed in table 1. Glass cells were used when pure PFBA was the solvent, to avoid a potential corrosion of the cells. When necessary, the mixtures of

Table 1: Details of the titration calorimetric experiments. The system PFBA + $[C_4C_1Im][OAc]$ was stopped after the first injections (see discussion part).

Perfluorobutyric acid			
Ionic liquid	Starting compositions in the cell (x_{PFBA})	Nb. of injections	T (K)
$[C_4C_1Im][OAc]$	0	6	313.15
$[C_2C_1Im][MeSO_3]$	0 / 0.03 / 0.25 / 0.4 / 0.8	29	313.15
$[C_4C_1Im][NTf_2]$	0 / 0.05 / 0.14 / 0.4 / 0.62 / 0.86 / 0.93 / 1	61	313.15
6:2 Fluorotelomer alcohol			
Ionic liquid	Starting compositions in the cell (x_{FTOH})	Nb. of injections	T (K)
$[C_2C_1Im][OAc]$	0.03 / 0.47	15	298.15
$[C_2C_1Im][MeSO_3]$	0.02 / 0.11 / 0.49 / 0.55	24	298.15
$[N_{222}H][MeSO_3]$	0.02 / 0.12 / 0.46 / 0.52	19	313.15

the ionic liquids and the fluorinated additives were prepared gravimetrically using a Mettler Toledo MS205DU precision balance. At room temperature and under argon atmosphere, 2 mL vials were filled without leaving any head space, to preserve the composition by avoiding evaporation of the F-substance. The compounds were mixed manually by the presence of glass spheres inside the vials and with mechanical stirring during 1 h at 250 rpm on a simple stirring plate.

The injections of solute into the sample cell were performed with a 250 µL gastight Hamilton syringe, with one of the pure compounds present in the syringe (the component of the mixture that was in minority in the cell). However, to avoid undesirable reactions when using pure PFBA, we have decided to fill the syringe, for the PFBA + $[C_2C_1Im][MeSO_3]$ system, with a mixture of a molar composition of 0.6 PFBA + 0.4 IL, which was injected into mixtures of 0.4 PFBA/0.6 IL and 0.8 PFBA/0.2 IL.

Prior to the first injection, the cannula connected to the syringe was immersed in the cell, just above the liquid, then inserted into the liquid when thermal equilibrium was reached, and finally electrical gain and dynamic calibrations were performed. Depending on the system, 1 to 10 µL injections were done by a motor driven pump (Thermometric 3810 Syringe Pump), during 30 seconds to 5 minutes, at intervals of time allowing for the return to the baseline of the signal after the additions. The heat effects appeared as peaks in the signal after each

injection and were integrated to quantify the heat Q, used to calculate the partial molar excess enthalpies $\overline{H}_i^E$ of the fluorinated substances and of the ionic liquids.

Results and discussion

In silico screening of ionic liquids

The surface charge density of **perfluorobutyric acid** (see figure 3) shows a very localised positive charge around the proton of the carboxy group (blue area) whereas the negative charge is spread between the oxygen atoms (red area). This charge distribution is clear in the σ-profile (see figure 4). $\sigma > 0$ corresponds to a positive surface charge of the cavity formed by the compounds, so to a negative surface charge of the compounds themselves. For PFBA, the peak corresponding to the negative charge is between 0.00 and 0.01 e/A^2, close to the dominant non-polar region. On the other hand, the positive charge is present at a more extreme value: -0.02 e/A^2. We can expect a large influence of the anions on the interactions of the ionic liquids with this solute. We can make the hypothesis of an acidic behaviour of PFBA, as the proton is likely to be the center of the interactions with basic components, confirmed by the very low pKa of the substance, *i.e.* 0.35 at 25°C.

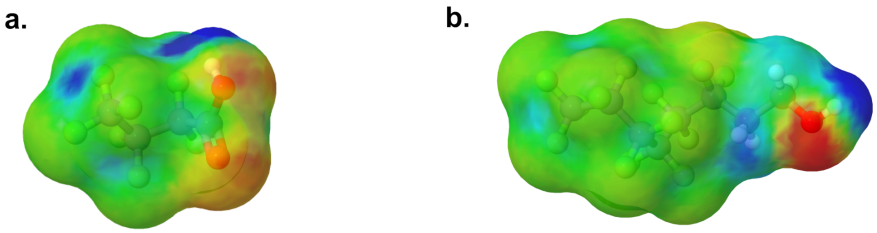

Figure 3: Surface charge densities of the studied PFAS, with a) PFBA and b) 6:2 FTOH.

The σ-profile and the surface charge density of **6:2 fluototelomer alcohol** show a more balanced behaviour, as both positive and negative charges are between -0.02 and 0.02 e/A^2, mainly localised on the hydroxy group. In the σ-profile, we can denote a slightly larger influence of the proton, close to the non-polar domain ($\sigma \approx -0.5e/A^2$). We can expect

here an equivalent influence of the cations and anions of the ionic liquids, the preferential interactions with one or another depending on the surface charge density of the ions.

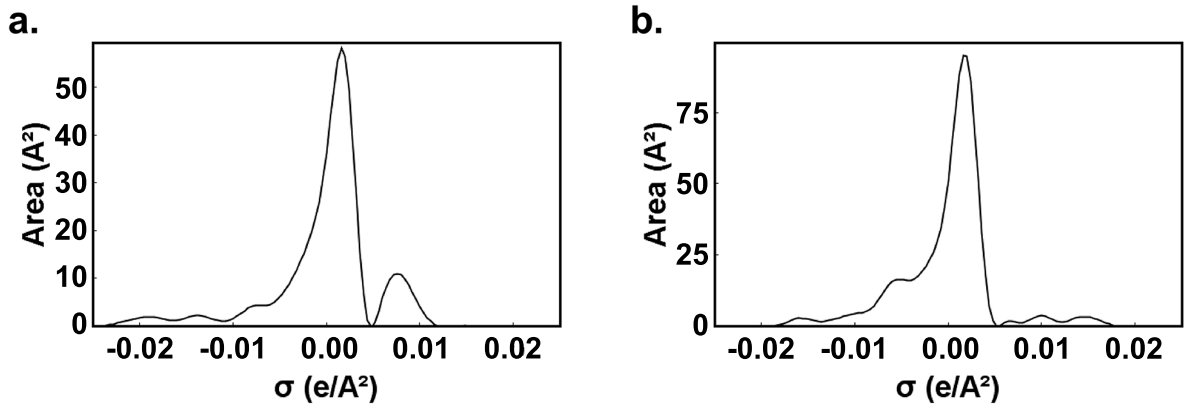

Figure 4: σ-profiles of the studied PFAS, with a) PFBA and b) 6:2 FTOH.

The screening of the infinite dilution activity coefficients for both perfluorobutyric acid and 6:2 fluorotelomer alcohol confirmed the preliminary conclusions drawn from the observation of the surface charge densities and σ-profiles. The two-way ANOVA without replication, made with the calculated $ln\gamma^{\infty}$ of the fluorinated acid in combinations of cations and anions representing potential ILs, showed a three times larger influence of the anion of the ionic liquid on the value of $ln\gamma^{\infty}$, and so on the interactions ($F_{anion} = 480$, $F_{cation} = 162$). Regarding the fluorinated alcohol, the anions and the cations had an equivalent influence ($F_{anion} = 118$, $F_{cation} = 110$).

For perfluorobutyic acid, negative value of $ln\gamma^{\infty} < 0$ (corresponding to favourable interactions) were found in 801 potential ionic liquids, while 6:2 fluorotelomer alcohol was expected to have an affinity for 244 potential ILs. For both substances, coloured maps, in supplementary information (Figures S1 and S2), show lower $ln\gamma^{\infty}$ in ILs with carboxylate or small anions such as $MeSO_3^-$, contrary to ILs with more hydrophobic or fluorinated anions. This is also observed for ammonium, imidazolium, pyridinium and pyrrolidinium, cations for which $ln\gamma^{\infty}$ increases with the size of the alkyl side-chains. This was already observed in previous works.[44]

Following these COSMO-SAC calculations, we focused our experimental measurements

for PFBA in imidazolium-based ($C_2C_1Im^+$ or $C_4C_1Im^+$) ILs and changed the anion, as it was supposed to have greater influence on the interactions. We selected two anions with the lowest $ln\gamma^\infty$, *i.e.* AcO^- and $MeSO_3^-$, and one which was expected to have less affinity but which was already used in F-gases capture, *i.e.* NTf_2^-. Therefore, $[C_4C_1Im][OAc]$, $[C_2C_1Im][MeSO_3]$ and $[C_4C_1Im][NTf_2]$ were identified and studied.

For 6:2 FTOH, the effect of both the cation and the anion was assessed, by selecting 3 ionic liquids: $[C_2C_1Im][OAc]$, $[C_2C_1Im][MeSO_3]$ and $[N_{222}H][MeSO_3]$. Note the presence of the ammonium-based protic ionic liquid, meaning that a proton exchange can take place between the cation and the anion. The calculated infinite dilution activity coefficients and the selected ionic liquids are displayed in table 2.

Table 2: Infinite dilution activity coefficients of PFBA and 6:2 FTOH in the selected ionic liquids for experimental measurements

Perfluorobutyric acid		**6:2 Fluorotelomer alcohol**	
Ionic liquid	$ln\gamma^\infty$	Ionic liquid	$ln\gamma^\infty$
$[C_4C_1Im][OAc]$	-3.342	$[C_2C_1Im][OAc]$	-0.275
$[C_2C_1Im][MeSO_3]$	-3.629	$[C_2C_1Im][MeSO_3]$	-0.563
$[C_4C_1Im][NTf_2]$	-0.371	$[N_{222}H][MeSO_3]$	-1.373

Mixing enthalpy

An example of calorimetric signal is shown in supplementary information (Figure S3), as well as the measured partial molar excess enthalpies $\overline{H}_i^E$, plotted along with the Redlich-Kister fitting (Figure S4 and S5).

Data interpretation for perfluorobutyric acid

Figure 5a shows the mixing enthalpy for systems with PFBA, and the absence of fitted results for the mixture PFBA + $[C_4C_1Im][OAc]$ should be noted. It is related with the low number of data points that could be measured (see table 1), in light of the unusually high heat released by the first injections of PFBA. For example, when 1 μL of pure PFBA was

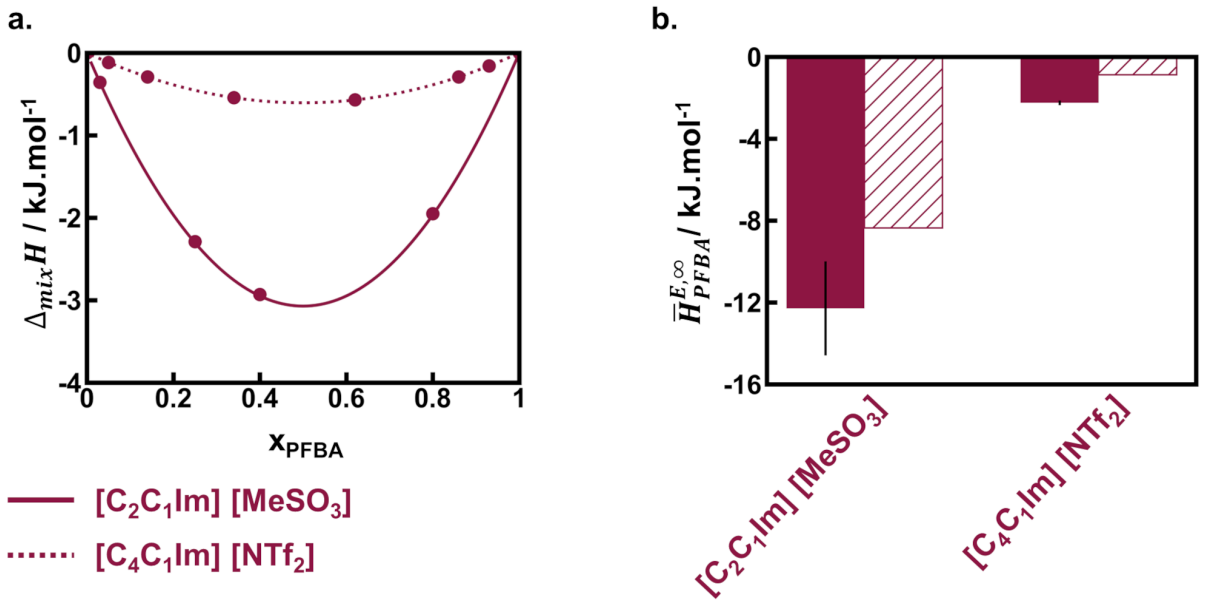

Figure 5: ITC results for PFBA (1 RK parameter), with a) the fitted mixing enthalpies (lines) and the measured compositions (circles) and b) the extrapolated $\overline{H}^{E,\infty}$ (plain bars) along with COSMO-SAC $RT.ln\gamma^{\infty}$ (hatched bars).

injected in 700 μL of pure [C_4C_1Im][OAc], the heat released was $Q = 610\ mJ$. For the same volume injected in pure [C_2C_1Im][$MeSO_3$] – the second IL showing the highest heat released – the heat was $Q = 90\ mJ$. We deduced that chemical or quasi-chemical interactions might be involved. Their accurate quantification requiring to inject PFBA in a larger quantity of IL, we decided to stop the experiment, as it would require to use significant amounts of IL. This large heat effect can probably be attributed to a proton exchange from PFBA to AcO^- anion, this phenomenon will be discussed later.

Only one RK (Redlich-Kister) parameter (A_0) was used to fit the data of the systems composed of PFBA with [C_4C_1Im][NTf_2] or [C_2C_1Im][$MeSO_3$]. In the case of [C_4C_1Im][NTf_2], a second parameter (A_1) in the RK fit would not significantly affect the precision of the fit or the uncertainty on $\overline{H}^{E,\infty}$ (4.5 $\%_{err}$ vs 6.7 $\%_{err}$, see table 3). Furthermore, A_1 itself had a higher uncertainty (18%) than A_0 (4%). Concerning [C_2C_1Im][$MeSO_3$], the combination of the uncertainties of two parameters resulted in a higher error for $\overline{H}^{E,\infty}_{PFBA}$ (75%) than when only one parameter was used (19%) (see table 3).

Table 3: Mixing enthalpy, RK parameters, infinite dilution partial molar excess enthalpy and COSMO-SAC activity coefficients, for PFBA in the studied ionic liquids. All the experimental values are in $kJ.mol^{-1}$.

One RK parameter							
Ionic liquid	$\Delta_{mix}H$	A_0	A_1	$\overline{H}^{E,\infty}_{PFBA}$	$\%_{err}$	$ln\gamma^{\infty}$	$RT.ln\gamma^{\infty}$
$[C_2C_1Im][MeSO_3]$	-3.1	-12 ± 2.3	-	-12 ± 2.3	19	-3.2	-8.4
$[C_4C_1Im][NTf_2]$	-0.6	-2.2 ± 0.1	-	-2.2 ± 0.1	4.5	-0.3	-0.9
Two RK parameters							
Ionic liquid	$\Delta_{mix}H$	A_0	A_1	$\overline{H}^{E,\infty}_{PFBA}$	$\%_{err}$	$ln\gamma^{\infty}$	$RT.ln\gamma^{\infty}$
$[C_2C_1Im][MeSO_3]$	-11	-40 ± 2.6	35 ± 3.0	-5.3 ± 4.0	75	-3.2	-8.4
$[C_4C_1Im][NTf_2]$	-0.7	-2.2 ± 0.1	-0.8 ± 0.1	-3.0 ± 0.2	6.7	-0.3	-0.9

Both systems showed negative mixing enthalpies (see figure 5), revealing favourable contributions to spontaneous mixing. In $[C_4C_1Im][NTf_2]$, the value for $x_{PFBA} = 0.5$ was $\Delta_{mix}H = -0.6\ kJ.mol^{-1}$ whereas we obtained $\Delta_{mix}H = -3.1\ kJ.mol^{-1}$ in $[C_2C_1Im][MeSO_3]$. However, the mixing enthalpy of PFBA+$[C_4C_1Im][NTf_2]$ was close to 0, so the deviation from ideality was small compared with PFBA+$[C_2C_1Im][MeSO_3]$. This observation highlights the fact that PFBA mixes more easily with ILs based on anions able to form H-bond interactions, like $MeSO_3^-$.

We could compare directly the values of extrapolated $\overline{H}^{E,\infty}_{PFBA}$ with the *in silico* screening. The activity coefficients can be linked to the Gibbs energy of mixing through the chemical potential μ_i of non-ideal mixtures:

$$\begin{aligned} \mu_i &= \mu_i^* + RT.lna_i \\ &= \mu_i^* + RT.lnx_i + RT.ln\gamma_i \\ \mu_i - \mu_i^* &= \left(\frac{\partial \Delta_{mix}G}{n_i}\right)_{p,T,n_{j\neq i}} \\ RT.ln\gamma_i &= \left(\frac{\partial \Delta_{mix}G}{n_i}\right)_{p,T,n_{j\neq i}} - RT.lnx_i \end{aligned} \tag{10}$$

where μ_i^* is the chemical potential of the pure compound and $a_i = x_i\gamma_i$ the activity of the compound in a non-ideal mixture.

Considering the definition of Gibbs energy, the approximation of ideal entropy of mixing,

$i.e\ \left(\frac{\partial \Delta_{mix} S}{n_i}\right)_{p,T,n_{j\neq i}} = lnx_i$, and the relation between mixing enthalpy and partial molar excess enthalpy (equation 4) we have:

$$\begin{aligned} RT.ln\gamma_i &= \left(\frac{\partial \Delta_{mix} H}{n_i}\right)_{p,T,n_{j\neq i}} \\ &= \left(\frac{\partial n H^E}{n_i}\right)_{p,T,n_{j\neq i}} \\ &= \overline{H}_i^E \end{aligned} \tag{11}$$

The COSMO-SAC infinite dilution activity coefficients $ln\gamma^{\infty}$ at $313.15K$ for PFBA in $[C_4C_1Im][NTf_2]$ and $[C_2C_1Im][MeSO_3]$ were -0.3 and -3.2, respectively, so a smaller deviation from ideality ($ln\gamma^{\infty} = 0$) was calculated for PFBA in $[C_4C_1Im][NTf_2]$. By extrapolation of equations 10 and 11, we could compare the COSMO-SAC calculated $RT.ln\gamma^{\infty}_{PFBA}$ with $\overline{H}^{E,\infty}_{PFBA}$ obtained from the RK fits (equation 9). Figure 5b shows that the behaviour at infinite dilution, so the energy $\overline{H}^{E,\infty}_{PFBA}$ due to the addition of one molecule of PFBA in only ion pairs, was correctly predicted by COSMO-SAC calcultations, as $\overline{H}^{E,\infty}_{PFBA}$ was much more negative in $[C_2C_1Im][MeSO_3]$ ($-12\ kJ.mol^{-1}$) than in $[C_4C_1Im][NTf_2]$ ($-2.2\ kJ.mol^{-1}$), the same being observed for $RT.ln\gamma^{\infty}_{PFBA}$.

Data interpretation for 6:2 fluorotelomer alcohol

Concerning mixtures with 6:2 FTOH, two RK parameters (A_0 and A_1) were used to fit the experimental data. For all ionic liquids, the experimental $\overline{H}_i^E$ were not well represented when using only A_0 (see Figure S5). Figure 6a shows that for this fluorinated substance, all mixing enthalpies were also negative, so contributing favourably to spontaneous mixing. The fact that for all ionic liquids the mixing enthalpy has the lowest value for $x_{FTOH} > 0.5$ means that adding IL to pure 6:2 FTOH released more energy than the other way around.

Note that our COSMO-SAC screening for 6:2 FTOH had shown that the calculated $ln\gamma^{\infty}$ were overall close to those of an ideal mixture, $-1 < ln\gamma^{\infty} < 0$ for all the selected ILs. We would have then expected to measure mixing enthalpies in the range of the values obtained

for PFBA in $[C_4C_1Im][NTf_2]$, *i.e.* close to 0. However, the experimental mixing enthalpy of 6:2 FTOH in $[C_2C_1Im][OAc]$ ($\Delta_{mix}H = -3.7\ kJ.mol^{-1}$) was higher than expected in light of the calculated activity coefficient, $ln\gamma^{\infty} = -0.3$, showing here a deviation between the prediction of the COSMO-SAC model and our experimental results.

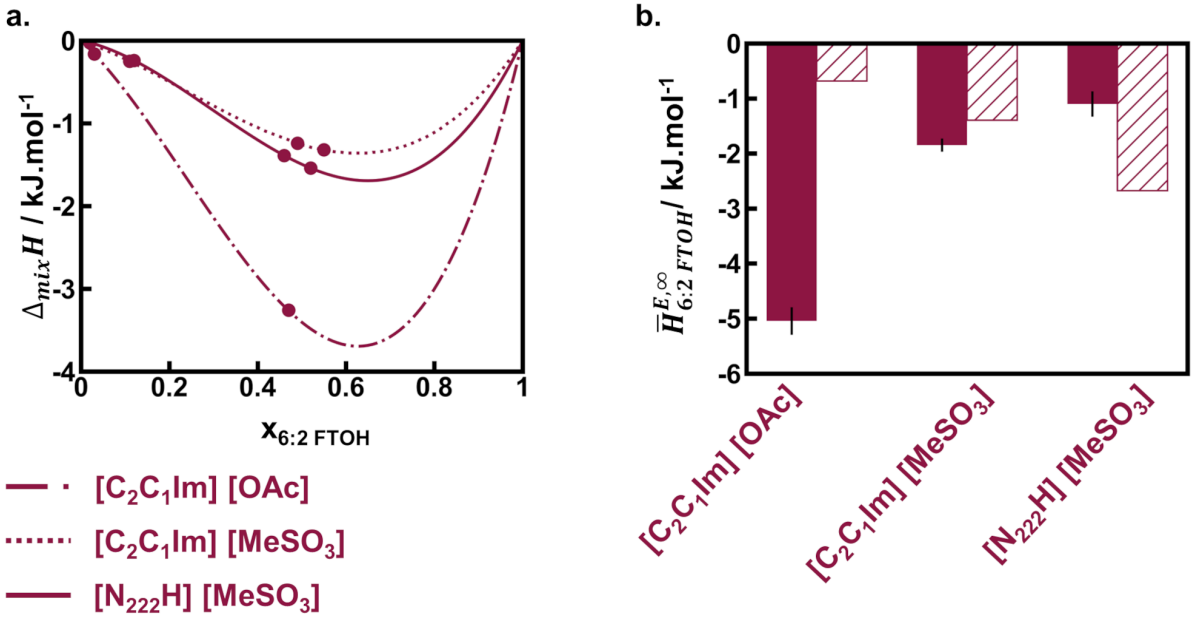

Figure 6: ITC results for 6:2 FTOH (2 RK parameters), with a) the fitted mixing enthalpies (lines) and the measured compositions (circles) and b) the extrapolated $\overline{H}^{E,\infty}$ (plain bars) along with COSMO-SAC $RT.ln\gamma^{\infty}$ (hatched bars).

This deviation between predicted and experimental results was not as marked with the $MeSO_3^-$ based ionic liquids, if only the values of mixing enthalpy are taken into consideration. With $[C_2C_1Im][MeSO_3]$, we measured a $\Delta_{mix}H$ of $-1.4\ kJ.mol^{-1}$ (calculated $ln\gamma^{\infty} = -0.6$) and with $[N_{222}H][MeSO_3]$, we determined experimentally a $\Delta_{mix}H$ of $-1.7\ kJ.mol^{-1}$ (calculated $ln\gamma^{\infty} = -1.0$). It highlights the fact that the change of cation did not make a deviation between the predicted and experimental results, whereas changing the anion from $MeSO_3^-$ to AcO^- involved non-expected more favourable interactions.

The values of $\overline{H}^{E,\infty}_{FTOH}$ in table 4, also displayed in figure 6b, show different trends when compared with COSMO-SAC $RT.ln\gamma^{\infty}$ predictions. Experimentally, when the medium does not contain any other molecule of F-alcohol, one molecule of 6:2 FTOH releases more en-

ergy when it interacts with $[C_2C_1Im][MeSO_3]$ ($\overline{H}^{E,\infty}_{FTOH} = -1.8\ kJ.mol^{-1}$) as compared with $[N_{222}H][MeSO_3]$ ($\overline{H}^{E,\infty}_{FTOH} = -1.1\ kJ.mol^{-1}$). This is a small difference in an already low value in comparison with some other mixtures of IL + associating compounds (e.g. alcohols or polar substances) reported in the literature,[43] but the opposite of what we expected from COSMO-SAC calculations ($RT.ln\gamma^{\infty} = -1.4$ in $[C_2C_1Im][MeSO_3]$ and $RT.ln\gamma^{\infty} = -2.7$ in $[N_{222}H][MeSO_3]$).

Table 4: Mixing enthalpy, RK parameters, infinite dilution partial molar excess enthalpy and COSMO-SAC activity coefficients, for 6:2 FTOH in the studied ionic liquids. All the experimental values are in $kJ.mol^{-1}$.

One RK parameter							
Ionic liquid	$\Delta_{mix}H$	A_0	A_1	$\overline{H}^{E,\infty}_{FTOH}$	$\%_{err}$	$ln\gamma^{\infty}$	$RT.ln\gamma^{\infty}$
$[C_2C_1Im][OAc]$	-2.0	-7.9 ± 1.2	-	-7.9 ± 1.2	15	-0.3	-0.7
$[C_2C_1Im][MeSO_3]$	-0.8	-3.1 ± 0.4	-	-3.1 ± 0.4	13	-0.6	-1.4
$[N_{222}H][MeSO_3]$	-1.1	-4.4 ± 0.9	-	-4.4 ± 0.9	20	-1.0	-2.7
Two RK parameters							
Ionic liquid	$\Delta_{mix}H$	A_0	A_1	$\overline{H}^{E,\infty}_{FTOH}$	$\%_{err}$	$ln\gamma^{\infty}$	$RT.ln\gamma^{\infty}$
$[C_2C_1Im][OAc]$	-3.7	-14 ± 0.2	8.6 ± 0.2	-5.0 ± 0.3	6.0	-0.3	-0.7
$[C_2C_1Im][MeSO_3]$	-1.4	-5.0 ± 0.1	3.2 ± 0.1	-1.8 ± 0.1	5.6	-0.6	-1.4
$[N_{222}H][MeSO_3]$	-1.7	-6.0 ± 0.1	4.9 ± 0.1	-1.1 ± 0.2	18	-1.0	-2.7

However, using two RK parameters as we did for these values is only valid when enough data are available all over the composition range, which was not the case here. Using both A_0 and A_1 allowed to assess the overall behaviour of the mixtures and to qualitatively conclude about mixing enthalpy ($\Delta_{mix}H$), but the approximation is larger at infinite dilution and using only A_0 allows a better description of the behaviour at these compositions.

Figure 7 depicts the partial molar excess enthalpy of 6:2 FTOH at infinite dilution using one (a) or two (b) RK parameters to fit the experimental data. Whereas COSMO-SAC calculations assessed an affinity order (namely $[N_{222}H][MeSO_3] > [C_2C_1Im][MeSO_3] > [C_2C_1Im][OAc]$) opposite to what was fitted with two RK parameters (Figure 7b), the order was the same using only A_0, considering the $MeSO_3^-$ based ILs (Figure 7a).

Nevertheless, the values of $\overline{H}^{E,\infty}_{FTOH}$ in each of the two ILs were in the same order of magnitude ($\overline{H}^{E,\infty}_{FTOH} = -3.1\ kJ.mol^{-1}$ in $[C_2C_1Im][MeSO_3]$ and $\overline{H}^{E,\infty}_{FTOH} = -4.4\ kJ.mol^{-1}$

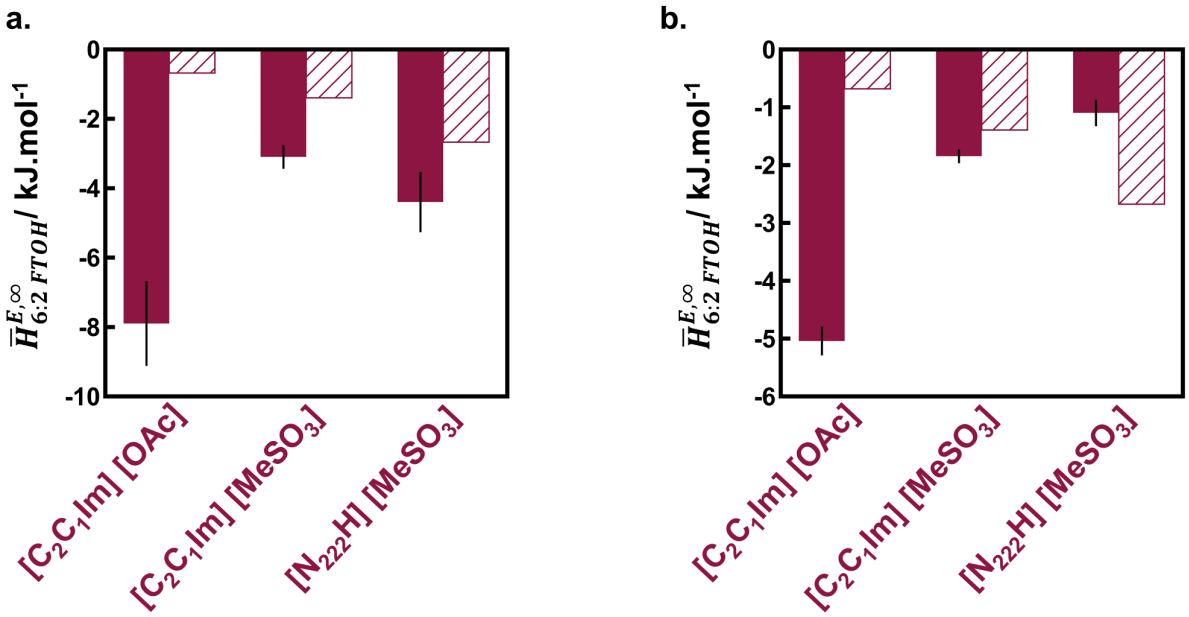

Figure 7: Extrapolation $\overline{H}^{E,\infty}$ (plain bars) along with COSMO-SAC $RT.ln\gamma^{\infty}$ (hatched bars) for 6:2 FTOH, using 1 RK parameter (a) or 2 RK parameters (b).

in [$N_{222}H$] [$MeSO_3$]) and both pointed to non-ideality. The partial molar excess enthalpy of 6:2 FTOH in [C_2C_1Im][OAc] at infinite dilution was still larger than what was expected from the COSMO-SAC calculations and than the other values of $\overline{H}^{E,\infty}$, pointing to specific interactions similar to those observed for PFBA in [C_4C_1Im][OAc].

Finally, in any case, the ITC measurements showed that the energy involved in interactions between 6:2 FTOH or PFBA and imidazolium acetate ionic liquids was much higher than our expectations, specially for PFBA. This implies that such ILs would be very interesting to retain these fluorinated substances during textile recycling, and it also shows that experimental measurements were needed to complement computational screening. The rationalization of the experimental data is also needed in such demanding experiments. Our results allowed to qualitatively determine the most interesting ionic liquids to test for the elimination of F-substances from textiles in view of their recycling. The interactions that could not be predicted using COSMO-SAC appeared experimentally with such intensity that pointed to specific mechanisms or even to proton exchange in mixtures with acetate ionic

liquids.

Investigation of a proton transfer from PFBA to [C_4C_1Im][OAc]

As we could not measure accurately the energy due to the interactions between PFBA and [C_4C_1Im][OAc], we tried to further investigate these mixtures by computational and spectroscopic characterization. Knowing that PFBA is a much stronger acid ($pK_a = 0.4$) than acetic acid ($pK_a = 4.8$), we suspected a proton transfer from PFBA to AcO^-.

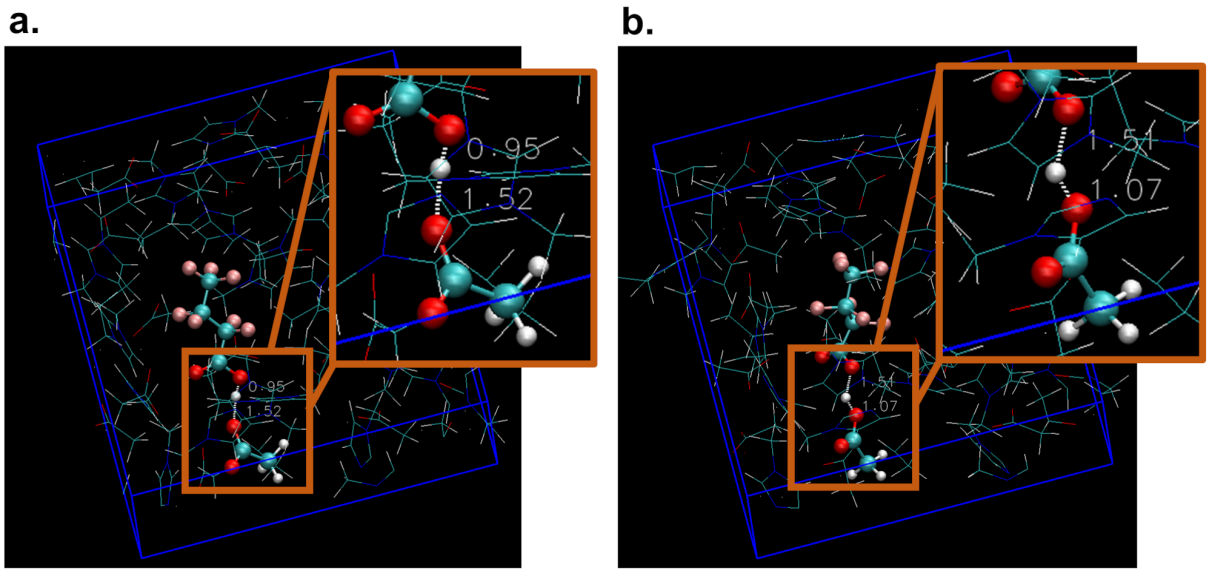

Figure 8: DFT calculations of the distance $O_{PFBA} - H - O_{Acetate}$ (a) at $t = 0$ fs and (b) $t = 100$ fs. PFBA is the upper molecule.

We started our investigation by simulating the system using *ab initio* molecular dynamics. DFT calculations were performed using the CP2K code with an explicit representation of the medium, composed of one molecule of PFBA in a periodic box with 20 [C_2C_1Im][OAc] ion pairs, at $353K$. In total, 400 configurations were simulated with a time step of 0.5 fs. Figure 8 shows the configuration at the beginning of the simulation and another one after 100 fs. The evolution of the $O_{PFBA} - H - O_{Acetate}$ distance over time is shown in supplementary information (Figure S6).

We observed that, when the simulation started, the proton was closer to PFBA ($d_{H-O_{PFBA}} =$

0.95Å) than the acetate ($d_{H-O_{acetate}} = 1.52$Å). After a short time during which the proton oscillated, it went closer to acetate ($d_{H-O_{acetate}} = 1.07$Å) and stabilised there (see figure 8b). Without any doubt, the simulation showed a proton transfer to occur spontaneously.

We have also performed ^1H NMR measurements of the pure compounds and of an equimolar mixture of PFBA and $[C_4C_1Im][OAc]$, prepared as described in the methods section and immediately characterised. We used benzene-d6 as deuterated solvent and ran the analysis with a Bruker spectrometer operating at 400 MHz. The NMR tubes were composed of a inner tube containing the solvent, inserted into a standard tube containing the species to be characterised. The tubes were prepared under argon atmosphere and the caps sealed with parafilm.

We could attribute each peak to a different proton (see figure 9 and table 5), confirmed by the literature,[45] and we only noticed two unknown impurities in $[C_4C_1Im][OAc]$, appearing as peaks at 2.15 ppm and 3.25 ppm. The spectrum of pure PFBA (see figure 9a) displays the only proton at 12.09 ppm, and we find also a single proton in this region, at 11.85 ppm, in the spectrum of the mixture (figure 9c). But, we cannot conclude that this proton is still part of PFBA.

We noticed that all the peaks corresponding to the protons of the imidazolium ring in pure IL (C_2, C_4, C_5 at $8.54-10.87$ ppm) were shifted to $7.79-9.46$ ppm in the mixture. This is a large shift which corresponds to an environment richer in electrons. In pure $[C_4C_1Im][OAc]$, the imidazolium ring is the site interacting with the anion. As it became richer in electrons, we can assume that, in the mixture with PFBA, the potentially deprotonated flurorinated acid (*i.e.* $C_3F_7COO^-$), richer in electrons than AcO^-, approached the imidazolium ring. Furthermore, the signal corresponding to $\mathbf{CH_3}-COO^-$ of acetate (C_{11}) was shifted to higher ppm. So its environment became less rich in electrons, which points to the presence of a proton connected to AcO^-.

We finally performed infrared spectroscopy measurements to investigate the possible proton transfer. The IR spectra of PFBA, $[C_4C_1Im][OAc]$ and a mixture of 0.5/0.5 mo-

Table 5: ^1H NMR identification for $[C_4C_1Im][OAc]$ as pure IL (a) and in mixture with PFBA (b), showing chemical shift δ, multiplicity M and integrals of the protons.

a. Pure $[C_4C_1Im][OAc]$				**b. PFBA + $[C_4C_1Im][OAc]$**			
H	δ (ppm)	M	Int.	H	δ (ppm)	M	Int.
9	0.84; 0.86; 0.88	t	3.05	9	0.94; 0.96; 0.98	t	3.00
8	1.22; 1.25; 1.26; 1.28; 1.29; 1.32	m	2.00	8	1.34; 1.35; 1.37; 1.39; 1.141; 1.43	m	2.01
11	1.80	s	3.25	7	1.88; 1.90; 1.92; 1.93; 1.95	s	2.05
7	1.85; 1.87; 1.88; 1.90; 1.92	m	2.02	11	2.01	m	3.18
10	4.21	s	3.06	10	4.06	s	2.94
6	4.47; 4.48; 4.50	t	2.00	6	4.33; 4.35; 4.37	t	1.97
4	8.54	s	1.03	4	7.79	s	1.00
5	8.69	s	0.98	5	7.88	s	0.98
2	10.87	s	0.98	2	9.46	s	0.99

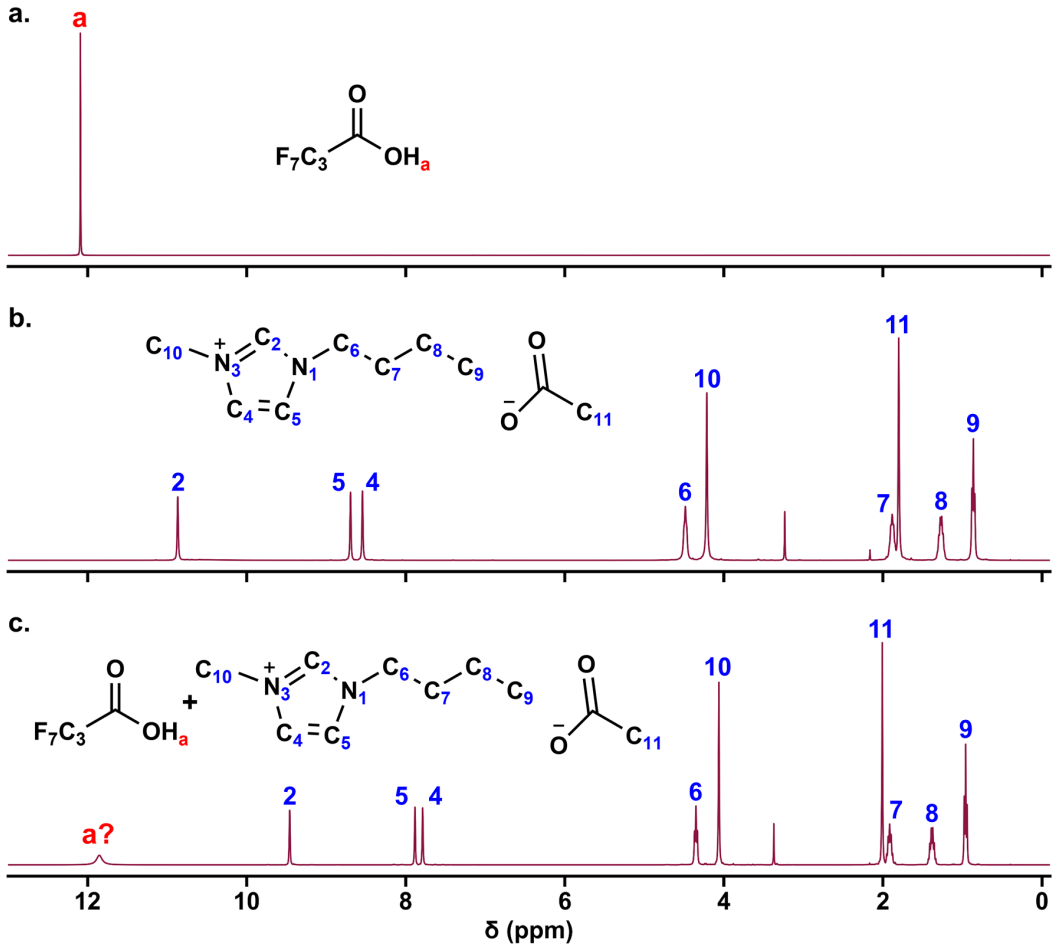

Figure 9: ^1H NMR spectra of a) pure PFBA, b) pure $[C_4C_1Im][OAc]$ and c) 0.5/0.5 molar mixture of PFBA and $[C_4C_1Im][OAc]$.

lar composition were collected in the attenuated total reflection mode (ATR) of a Perkin Elmer Spectrum 65 FTIR spectrometer. A droplet of each sample was placed on top of the ATR crystal, and the measurements were performed in order to accumulate 64 scans in the wavenumber range of 515 cm^{-1} to 4000 cm^{-1} with 2 cm^{-1} of resolution. The spectra are fully displayed in supplementary information (Figure S7). Figure 10 shows the signal obtained between 1500 cm^{-1} and 1900 cm^{-1}.

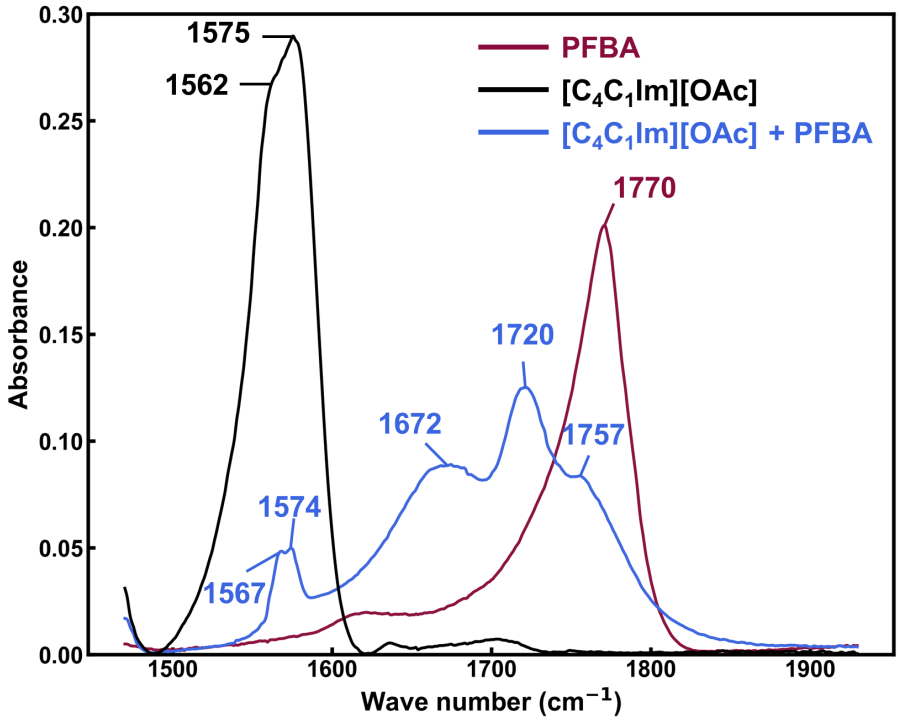

Figure 10: FT Infrared spectrum of pure PFBA (red), pure $[C_4C_1Im][OAc]$ (black) and 0.5/0.5 molar mixture of PFBA and $[C_4C_1Im][OAc]$ (blue), focused on the area $1500 - 1900$ cm^{-1}.

The analysis of the pure compounds allowed us to identify the band of the protonated COOH bond in PFBA (1770 cm^{-1}, red) and the COO^- bond of the acetate anion (range $1562 - 1575$ cm^{-1}, black). The spectrum of the mixture shows two supplementary bands. Thanks to the spectra of the pure compounds, we could attribute again the band at 1757 cm^{-1} to $COOH_{PFBA}$ and the band at $1567 - 1574$ cm^{-1} to $COO^-_{Acetate}$.

The two other bands show a change of the vibration frequency of COO bond, involved by the interactions between the substances. This change is usually due to a movement of

the proton H. According to the Spectral Database for Organic Compounds SDBS,[46] the typical COOH bond of acetic acid appears at 1715 cm^{-1}, that we can match with the band at 1720 cm^{-1} in our mixture. If we consider trifluoroacetic acid (CF_3COOH) as an example of fluorinated compound similar to PFBA, whose we have data in the SDBS database, the band of the acid ($\sigma_{COOH} = 1783\ cm^{-1}$) is shifted by 90 cm^{-1}, to $\sigma_{COO^-} = 1693\ cm^{-1}$ when it looses its proton. We find an equivalent shift in the signal of PFBA, with a band at 1672 cm^{-1} in the mixture (shifted from 1770 cm^{-1} in pure PFBA), showing the deprotonation of the fluorinated acid.

We can conclude what we observed with DFT calculations, and discerned with NMR spectroscopy, *i.e.* there is a proton transfer from PFBA to AcO^-. The original substances are still present in the mixture, as we can see their corresponding bands in the FTIR spectrum, because there is an equilibrium between the different conformations of the COO bond. These chemical interactions explain the generation of a high calorimetric response when mixing with $[C_4C_1Im][OAc]$. A similar behaviour was observed when mixing 6:2 FTOH with $[C_2C_1Im][OAc]$, but not with $[C_2C_1Im][MeSO_3]$, so we can assume that this phenomenon is related with the larger H-bond basicity of the acetate anion.[47]

Conclusions

We could measure the energy related to the interactions between PFBA or 6:2 FTOH and selected ionic liquids. As COSMO-SAC calculations of $ln\gamma^{\infty}_{PFAS}$ could hint, the mixing enthalpies of PFBA and 6:2 FTOH with all the ILs were negative, pointing to favourable interactions between the components. Moreover, we could predict that the anions had the highest influence on the affinity between PFAS and ILs. For both substances, anions with higher H-bond basicity, such as AcO^- and to a lesser extent $MeSO_3^-$, involved larger deviations from ideality. Acetate ionic liquids were particularly interesting, as a proton exchange within the mixture made the affinity stronger.

References

(1) Schellenberger, S.; Hill, P. J.; Levenstam, O.; Gillgard, P.; Cousins, I. T.; Taylor, M.; Blackburn, R. S. Highly fluorinated chemicals in functional textiles can be replaced by re-evaluating liquid repellency and end-user requirements. *Journal of Cleaner Production* **2019**, *217*, 134–143.

(2) KEMI, *Occurrence and use of highly fluorinated substances and alternatives. Report from a government assignment*; 2015; Vol. 7/15.

(3) Wang, Z.; Dewitt, J. C.; Higgins, C. P.; Cousins, I. T. A Never-Ending Story of Per- and Polyfluoroalkyl Substances (PFASs)? *Environmental Science and Technology* **2017**, *51*, 2508–2518.

(4) Song, K.; Lee, J.; Choi, S. O.; Kim, J. Interaction of surface energy components between solid and liquid on wettability. *Polymers* **2019**, *11*.

(5) Buck, R. C.; Franklin, J.; Berger, U.; Conder, J. M.; Cousins, I. T.; Voogt, P. D.; Jensen, A. A.; Kannan, K.; Mabury, S. A.; van Leeuwen, S. P. Perfluoroalkyl and polyfluoroalkyl substances in the environment: Terminology, classification, and origins. *Integrated Environmental Assessment and Management* **2011**, *7*, 513–541.

(6) Lassen, C.; Kjølholt, J.; Hagen Mikkelsen, S.; Warming, M.; Jensen, A. A.; Bossi, R.; Bondgaard, I. *Polyfluoroalkyl substances (PFASs) in textiles for children*; 2015.

(7) Prevedouros, K.; Cousins, I. T.; Buck, R. C.; Korzeniowski, S. H. Sources, fate and transport of perfluorocarboxylates. *Environmental Science and Technology* **2006**, *40*, 32–44.

(8) Schellenberger, S.; Jönsson, C.; Mellin, P.; Levenstam, O. A.; Liagkouridis, I.; Ribbenstedt, A.; Hanning, A. C.; Schultes, L.; Plassmann, M. M.; Persson, C.; Cousins, I. T.; Benskin, J. P. Release of Side-Chain Fluorinated Polymer-Containing Microplastic

Fibers from Functional Textiles during Washing and First Estimates of Perfluoroalkyl Acid Emissions. *Environmental Science and Technology* **2019**, *53*, 14329–14338.

(9) Holmquist, H.; Schellenberger, S.; van der Veen, I.; Peters, G. M.; Leonards, P. E.; Cousins, I. T. Properties, performance and associated hazards of state-of-the-art durable water repellent (DWR) chemistry for textile finishing. *Environment International* **2016**, *91*, 251–264.

(10) van der Veen, I.; Hanning, A. C.; Stare, A.; Leonards, P. E.; de Boer, J.; Weiss, J. M. The effect of weathering on per- and polyfluoroalkyl substances (PFASs) from durable water repellent (DWR) clothing. *Chemosphere* **2020**, *249*, 126100.

(11) Schellenberger, S.; Liagkouridis, I.; Awad, R.; Khan, S.; Plassmann, M.; Peters, G.; Benskin, J. P.; Cousins, I. T. An Outdoor Aging Study to Investigate the Release of Per- and Polyfluoroalkyl Substances (PFAS) from Functional Textiles. *Environmental Science and Technology* **2022**, *56*, 3471–3479.

(12) Cousins, I. T.; Dewitt, J. C.; Glüge, J.; Goldenman, G.; Herzke, D.; Lohmann, R.; Ng, C. A.; Scheringer, M.; Wang, Z. The high persistence of PFAS is sufficient for their management as a chemical class. *Environmental Science: Processes and Impacts* **2020**, *22*, 2307–2312.

(13) Ahrens, L.; Shoeib, M.; Harner, T.; Lee, S. C.; Guo, R.; Reiner, E. J. Wastewater treatment plant and landfills as sources of polyfluoroalkyl compounds to the atmosphere. *Environmental Science and Technology* **2011**, *45*, 8098–8105.

(14) Wild, S.; McLagan, D.; Schlabach, M.; Bossi, R.; Hawker, D.; Cropp, R.; King, C. K.; Stark, J. S.; Mondon, J.; Nash, S. B. An antarctic research station as a source of brominated and perfluorinated persistent organic pollutants to the local environment. *Environmental Science and Technology* **2015**, *49*, 103–112.

(15) Macorps, N.; Le Menach, K.; Pardon, P.; Guérin-Rechdaoui, S.; Rocher, V.; Budzinski, H.; Labadie, P. Bioaccumulation of per- and polyfluoroalkyl substance in fish from an urban river: Occurrence, patterns and investigation of potential ecological drivers. *Environmental Pollution* **2022**, *303*.

(16) Vierke, L.; Staude, C.; Biegel-Engler, A.; Drost, W.; Schulte, C. Perfluorooctanoic acid (PFOA)-main concerns and regulatory developments in Europe from an environmental point of view. *Environmental Sciences Europe* **2012**, *24*, 1–11.

(17) Borg, D.; Lund, B. O.; Lindquist, N. G.; Håkansson, H. Cumulative health risk assessment of 17 perfluoroalkylated and polyfluoroalkylated substances (PFASs) in the Swedish population. *Environment International* **2013**, *59*, 112–123.

(18) EU, Directive 2006/118/EC of the European Parliament and of the Council of 12 December 2006 on the protection of groundwater against pollution and deterioration. *Official Journal of the European Union* **2006**, *372*, 19–31.

(19) EU, Commission Regulation (EU) 2017/1000 of 13 June 2017 amending Annex XVII to Regulation (EC) No 1907/2006 of the European Parliament and of the Council concerning the Registration, Evaluation, Authorisation and Restriction of Chemicals (REACH) as regards perfluorooctanoic acid (PFOA), its salts and PFOA-related substances. *Official Journal of the European Union* **2017**,

(20) EU, Commission Regulation (EU) 2021/1297 of 4 August 2021 amending Annex XVII to Regulation (EC) No 1907/2006 of the European Parliament and of the Council as regards perfluorocarboxylic acids containing 9 to 14 carbon atoms in the chain (C9-C14 PFCAs), their. *Official Journal of the European Union* **2021**,

(21) Foster, A.; Environment, W.; Gmbh, I.; Group, W.; Wood, R. W.; Wood, L. N.; Wood, I. K.; Wood, J. K.; Pfa, M. C. The use of PFAS and fluorine-free alternatives in textiles , upholstery , carpets , leather and apparel. **2020**,

(22) Schellenberger, S.; Gillgard, P.; Stare, A.; Hanning, A.; Levenstam, O.; Roos, S.; Cousins, I. T. Facing the rain after the phase out: Performance evaluation of alternative fluorinated and non-fluorinated durable water repellents for outdoor fabrics. *Chemosphere* **2018**, *193*, 675–684.

(23) Welton, T. Ionic liquids: a brief history. *Biophysical Reviews* **2018**, *10*, 691–706.

(24) MacFarlane, D.; Kar, M.; Pringle, J. *Fundamentals of Ionic Liquids - From Chemistry to Applications*; Wiley-VCH, 2017; p 248.

(25) Greer, A. J.; Jacquemin, J.; Hardacre, C. Industrial Applications of Ionic Liquids. *Molecules (Basel, Switzerland)* **2020**, *25*, 1–31.

(26) Isosaari, P.; Srivastava, V.; Sillanpää, M. Ionic liquid-based water treatment technologies for organic pollutants: Current status and future prospects of ionic liquid mediated technologies. *Science of The Total Environment* **2019**, *690*, 604–619.

(27) Sovacool, B. K.; Griffiths, S.; Kim, J.; Bazilian, M. Climate change and industrial F-gases: A critical and systematic review of developments, sociotechnical systems and policy options for reducing synthetic greenhouse gas emissions. *Renewable and Sustainable Energy Reviews* **2021**, *141*, 110759.

(28) Pison, L.; Canongia Lopes, J. N.; Rebelo, L. P.; Padua, A. A.; Costa Gomes, M. F. Interactions of fluorinated gases with ionic liquids: Solubility of CF 4, C2F6, and C3F8 in trihexyltetradecylphosphonium bis(trifluoromethylsulfonyl)amide. *Journal of Physical Chemistry B* **2008**, *112*, 12394–12400.

(29) Sosa, J. E.; Ribeiro, R. P.; Castro, P. J.; Mota, J. P.; Araújo, J. M.; Pereiro, A. B. Absorption of Fluorinated Greenhouse Gases Using Fluorinated Ionic Liquids. *Industrial and Engineering Chemistry Research* **2019**, *58*, 20769–20778.

(30) Sosa, J. E.; Santiago, R.; Hospital-Benito, D.; Costa Gomes, M.; Araújo, J. M.; Pereiro, A. B.; Palomar, J. Process Evaluation of Fluorinated Ionic Liquids as F-Gas Absorbents. *Environmental Science and Technology* **2020**, *54*, 12784–12794.

(31) Zhang, K.; Kujawski, D.; Spurrell, C.; Wang, D.; Yan, J.; Crittenden, J. C. Extraction of PFOA from dilute wastewater using ionic liquids that are dissolved in N-octanol. *Journal of Hazardous Materials* **2021**, *404*, 124091.

(32) Grabda, M.; Zawadzki, M.; Oleszek, S.; Matsumoto, M.; Królikowski, M.; Tahara, Y. Removal of Perfluorooctanoic Acid from Water Using a Hydrophobic Ionic Liquid Selected Using the Conductor-like Screening Model for Realistic Solvents. *Environmental Science and Technology* **2021**,

(33) Zhang, K.; Kujawski, D.; Spurrell, C.; Wang, B.; Crittenden, J. C. Screening ionic liquids for efficiently extracting perfluoroalkyl chemicals (PFACs) from wastewater. *Journal of Environmental Sciences (China)* **2023**, *127*, 866–874.

(34) Jaschik, M.; Piech, D.; Warmuzinski, K.; Jaschik, J. Prediction of Gas Solubility in Ionic Liquids Using the Cosmo-Sac Model. *Chemical and Process Engineering* **2017**, *38*, 19–30.

(35) Yang, L.; Sandler, S. I.; Peng, C.; Liu, H.; Hu, Y. Prediction of the phase behavior of ionic liquid solutions. *Industrial and Engineering Chemistry Research* **2010**, *49*, 12596–12604.

(36) Lee, B.-S.; Lin, S.-T. The role of long-range interactions in the phase behavior of ionic liquids. *Physical Chemistry Chemical Physics* **2012**, *14*, 6520.

(37) Guo, Z.; Lue, B. M.; Thomasen, K.; Meyer, A. S.; Xu, X. Predictions of flavonoid solubility in ionic liquids by COSMO-RS: Experimental verification, structural elucidation, and solvation characterization. *Green Chemistry* **2007**, *9*, 1362–1373.

(38) Mutelet, F.; Alonso, D.; Stephens, T. W.; Acree, W. E.; Baker, G. A. Infinite dilution activity coefficients of solutes dissolved in two trihexyl(tetradecyl)phosphonium ionic liquids. *Journal of Chemical and Engineering Data* **2014**, *59*, 1877–1885.

(39) Lee, B.-s.; Lin, S.-t. Prediction and screening of solubility of pharmaceuticals in single- and mixed-ionic liquids using COSMO-SAC model. *AIChE Journal* **2017**, *63*, 3096–3104.

(40) Klamt, A. Conductor-like screening model for real solvents: A new approach to the quantitative calculation of solvation phenomena. *Journal of Physical Chemistry* **1995**, *99*, 2224–2235.

(41) Lin, S. T.; Sandler, S. I. A priori phase equilibrium prediction from a segment contribution solvation model. *Industrial and Engineering Chemistry Research* **2002**, *41*, 899–913.

(42) Gerber, R. P.; Soares, R. D. P. Prediction of infinite-dilution activity coefficients using UNIFAC and COSMO-SAC variants. *Industrial and Engineering Chemistry Research* **2010**, *49*, 7488–7496.

(43) Podgoršek, A.; Jacquemin, J.; Pádua, A. A.; Costa Gomes, M. F. Mixing Enthalpy for Binary Mixtures Containing Ionic Liquids. *Chemical Reviews* **2016**, *116*, 6075–6106.

(44) Ferreira, R.; Blesic, M.; Trindade, J.; Marrucho, I.; Lopes, J. N.; Rebelo, L. P. N. Solubility of fluorinated compounds in a range of ionic liquids. Cloud-point temperature dependence on composition and pressure. *Green Chemistry* **2008**, *10*, 918–92.

(45) Besnard, M.; Cabaço, M. I.; Vaca Chávez, F.; Pinaud, N.; Sebastião, P. J.; Coutinho, J. A.; Mascetti, J.; Danten, Y. CO2 in 1-butyl-3-methylimidazolium acetate. 2. NMR investigation of chemical reactions. *Journal of Physical Chemistry A* **2012**, *116*, 4890–4901.

(46) AIST (National Institute of Advanced Industrial Science and Technology), SDBS Web. `https://sdbs.db.aist.go.jp`.

(47) Cláudio, A. F. M.; Swift, L.; Hallett, J. P.; Welton, T.; Coutinho, J. A.; Freire, M. G. Extended scale for the hydrogen-bond basicity of ionic liquids. *Physical Chemistry Chemical Physics* **2014**, *16*, 6593–6601.